

Reynolds number required to accurately discriminate between trends of skin friction and streamwise peak intensities in wall turbulence

Hassan Nagib*

ILLINOIS TECH (IIT), Chicago, IL 60616, USA

Peter Monkewitz†

École Polytechnique Fédérale de Lausanne (EPFL), CH-1015 Lausanne, Switzerland

Katepalli R. Sreenivasan‡

Tandon School of Engineering, Courant Institute of Mathematical Sciences,
Department of Physics, New York University, New York, USA

(Dated: September 18, 2024)

We expand on the conclusion of Nagib, Chauhan & Monkewitz [1] that nearly all available skin friction relations for zero-pressure-gradient turbulent boundary layers come into remarkable agreement over the entire range $Re_\theta < O(10^8)$, where Re_θ is the momentum thickness Reynolds number, provided one coefficient is adjusted in each relation by anchoring it to the most accurate measurements known. Regarding the peak of the streamwise turbulence intensity we find good agreement between the three analyses of Monkewitz [2], Chen & Sreenivasan [3] and Monkewitz & Nagib [4], with some coefficients slightly modified. We conclude that, several existing comparisons notwithstanding, accurate measurements in flows with $Re_\tau > O(10^6)$, where Re_τ is the friction Reynolds number, are required to *directly* discriminate between the existing theories of Marusic & Monty (2019) [5] and Chen & Sreenivasan [3].

Purpose of the note: Our goal here is to add to the discussion on the important topic of the asymptotic behavior of streamwise turbulent stress peaks in the wall layer. In particular, we estimate the Reynolds numbers needed for a *direct* assessment of the two competing theoretical results for the behavior of the variance. To do this properly, we first need to ascertain the accuracy of available measurements of skin friction and the Reynolds number. Accordingly, we organize the paper into two sections—accuracy of available skin friction data, and the mean square values of streamwise fluctuations in the wall layer—and present a conclusion.

Skin friction in turbulent boundary layers: For over a century, several relations have been proposed to describe the skin friction coefficient in zero pressure gradient (ZPG) turbulent boundary layers (TBLs). The differences between them can be as much as 20% to 40% as reflected in the top part of figure 1. In most cases these empirical correlations are not based on rigorous analysis and often lack even the empirical underpinning by accurate experimental data, or are based on observations from boundary layers that are not in strict ZPG conditions. About two decades ago the availability of the oil film interferometry to measure wall-shear stress with an accuracy in the order of 1.5% has allowed measurements in the facilities at ILLINOIS TECH (IIT), Chicago, and in KTH, Stockholm, over wide range of Reynolds numbers in accurately established ZPG conditions—i.e., with variations of freestream velocity of the order of 0.2%. The data from these two experiments are included in the present figure 1 and in Nagib, Chauhan & Monkewitz (2007) [1], and none of the existing relations in the literature is in good agreement with the data.

A table reproduced as figure 2 summarizes the various skin friction coefficients C_f , found in the literature as a function of the momentum thickness Reynolds number, Re_θ , identified as “original form”. Fitting each of the relations to the measured skin friction using oil film interferometry, while allowing only one coefficient, marked with bold text in the figure, adjusted using a least-squares algorithm, yields the “modified” coefficients listed in the table. Note that the Coles-Fernholz relations were fitted directly to the data, with the coefficient κ and the additive constant included in the figure. The bottom part of figure 1 shows remarkable agreement between all the “modified” relations including the Coles-Fernholz relations.

Extrapolating all the “modified” relations up to Re_θ of 10^{20} in figure 3, we find the differences to be 20% at $Re_\theta = 10^8$ and about 40% at $Re_\theta = 10^{16}$. Even at “galactic” Reynolds numbers of 10^{16} , the differences between all relations are comparable to their differences in the “original form” at Re_θ around 10^4 . At present, we believe that this relation best describes the skin friction coefficient towards asymptotically high Reynolds numbers.

Peak in the streamwise fluctuation intensity: Recently, with the growth of the direct numerical simulations (DNS) data base, the high Reynolds number trends of streamwise fluctuations in wall-bounded turbulence have received increasing attention. One focus has been the Re_τ -trend near the wall of the peak in intensity of the streamwise

* nagib@iit.edu

† peter.monkewitz@epfl.ch

‡ katepalli.sreenivasan@nyu.edu

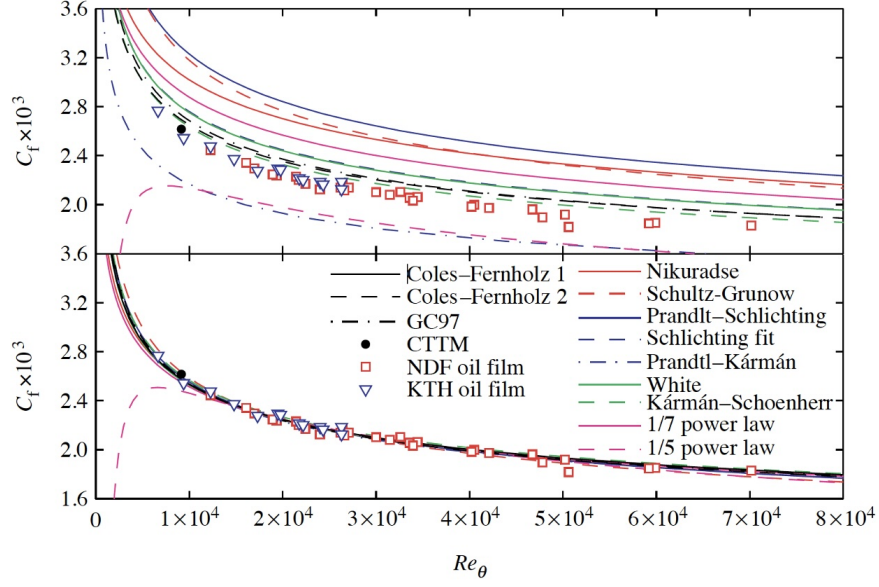


FIG. 1: Reproduction of figure 1 of Nagib, Chauhan & Monkewitz (2007) [1]: Variation of skin-friction coefficient with Re_θ . Experimental data from NDF and KTH are compared with relations for ZPG TBLs found in the literature.

component of the fluctuation velocity, $\langle uu \rangle_P^+$. In the following, we compare the observed trends with the finite limit at infinite Reynolds number based on the boundedness of dissipation (Chen & Sreenivasan [3, 6]) and the logarithmic unbounded growth as predicted by the attached eddy model founded on Townsend's hypothesis (e.g., Marusic & Monty (2019) [5]). In particular, Chen & Sreenivasan concluded that the near-wall peaks in the variance of the fluctuations are bounded for large Re_τ according to the relation

$$\langle uu \rangle_P^+ = 11.5 - 19.3 Re_\tau^{-0.25}. \quad (1)$$

The relevant results from their work are presented in figure 4, with the figure caption providing the data sources. In the spirit of the discussion on the skin friction, two coefficients in the proposed relation can be adjusted slightly to match those from Monkewitz [2]:

$$\langle uu \rangle_P^+ = 11.3 - 17.7 Re_\tau^{-0.25}. \quad (2)$$

A formula from Monkewitz & Nagib (2015) has the form

$$\langle uu \rangle_P^+ = 12.8 - \frac{80 \kappa}{\ln Re_\tau}. \quad (3)$$

The constants in (3) are somewhat different in the authors' original work. Their readjustment in the formula is done here only to explore if (3) can be brought in agreement with (2) merely by readjusting the constants without changing the functional form.

In figure 6, equations 2 and 3 are compared over a wide range of Re_τ to the proposed relations of Marusic et al. (2015) [15]:

$$\langle uu \rangle_P^+ = 0.63 \ln Re_\tau + 3.8, \quad (4)$$

and the relation of Samie et al. (2018) [17]:

$$\langle uu \rangle_P^+ = 0.646 \ln Re_\tau + 3.54. \quad (5)$$

It appears that the saturation formula fits the data somewhat better. There are other tests (see Nagib, Vinuesa & Hoyas (2024) [24], especially figures 3 and 5) that favor the saturation with the $-1/4$ power, but a direct test of the variance is only as good as in figure 4 here. This is the reason for the present effort to determine how high an Re_τ is required to see the differences directly and unambiguously. It should also be pointed that, while three plausible

relation by	original form	modified
Coles–Fernholz 1	$C_f = 2[1/\kappa \ln(Re_\theta) + C^*]^{-2}$	$\kappa=0.384, C^*=3.354$
Coles–Fernholz 2	$C_f = 2[1/\kappa \ln(Re_\theta) + C]^{-2}$	$\kappa=0.384, C=4.127$
Kármán–Schoenherr	$C_f = 0.558 C_f' / [0.558 + 2(C_f')^{-1/2}]$ $C_f' = [\log(2Re_\theta) / \mathbf{0.242}]^{-2}$	0.2385
Prandtl–Schlichting	$C_f = \mathbf{0.455} (\log Re_x)^{-2.58} - A/Re_x$	0.3596
Prandtl–Kármán	$C_f^{-1/2} = 4 \log(Re_x \sqrt{C_f}) - \mathbf{0.4}$	2.12
F. Schultz-Grunow	$C_f = \mathbf{0.427} (\log Re_x - 0 : 407)^{-2.64}$	0.3475
Nikuradse	$C_f = 0.02666 Re_x^{-0.139}$	-0.1502
Schlichting's fit	$C_f = (2 \log Re_x - 0.65)^{-2.3}$	-2.3333
White	$C_f = \mathbf{0.455} [\ln(0.06 Re_x)]^{-2}$	0.4177
1/7th law	$C_f = \mathbf{0.027} Re_x^{-1/7}$	0.02358
1/5th law	$C_f = \mathbf{0.058} Re_x^{-1/5} - A/Re_x$	0.0655
GC97	$C_f^{1/2} = 2(\mathbf{55} / C_{i\infty} [\delta^+]^{-\gamma_\infty} \exp[A/(\ln \delta^+)^\alpha])$	56.7

FIG. 2: The figure reproduces an image of table 1 of Nagib, Chauhan & Monkewitz (2007) [1]: Skin-friction relations used to fit the KTH and NDF oil-film data in figure 1. (Throughout the table, x is the downstream distance measured from the leading edge.)

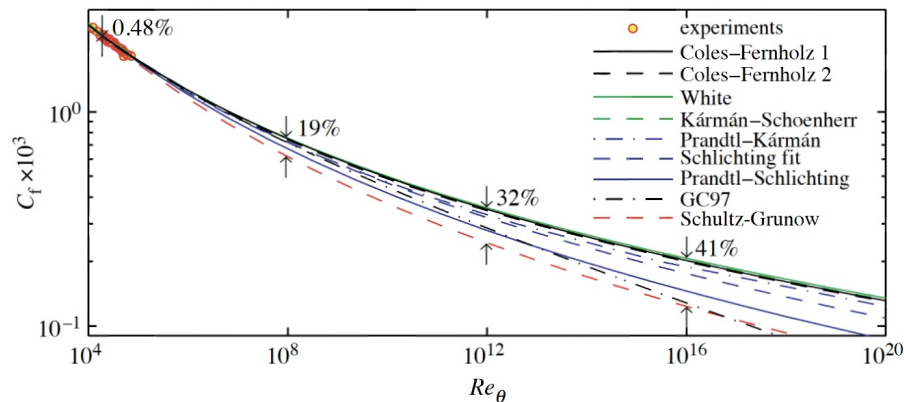


FIG. 3: Reproduction of figure 2 of Nagib, Chauhan & Monkewitz (2007) [1]: Asymptotic behaviour of modified C_f relations and their local deviations.

theoretical underpinnings of the saturation result were advanced in [3, 6], each of them has an empirical content. An example of a promising direction of future research is the investigation of Smits et al. (2021) [25], where the Reynolds number dependence of the leading coefficient of the Taylor expansion of $\langle uu \rangle^+$ about the wall is investigated among other quantities. The Re_τ dependence of the four Taylor coefficients for the channel in their Table 1 are least-squares fitted by

$$\frac{\langle uu \rangle^+}{(y^+)^2} (y^+ \rightarrow 0) = 0.0157 \ln Re_\tau + 0.0660 \quad (6)$$

with $R^2 = 0.991$ and an average deviation of 0.67% (0.98% maximum) from the fit. The alternate fit, not explored by Smits et al. (2021) [25] is

$$\frac{\langle uu \rangle^+}{(y^+)^2} (y^+ \rightarrow 0) = 0.246 - 0.400 Re_\tau^{-1/4} \quad (7)$$

with $R^2 = 1.000$ and an average deviation of 0.13% (0.26% maximum) from the fit. There is little doubt that the data support the asymptotic result of about 0.25 for $\frac{\langle uu \rangle^+}{(y^+)^2}$.

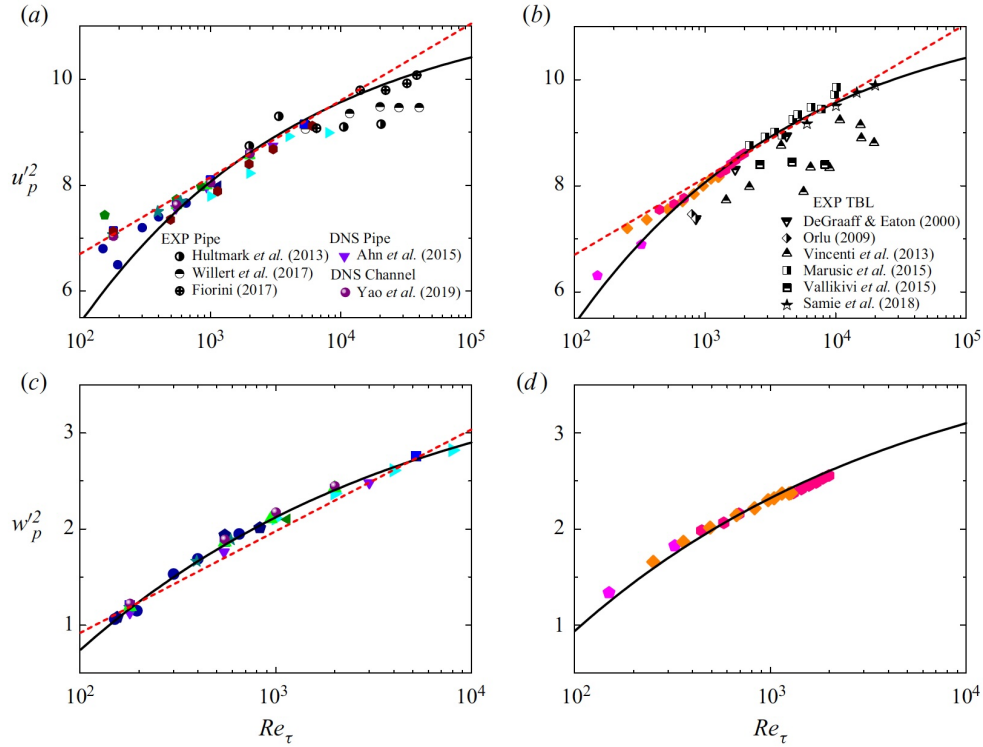


FIG. 4: Reproduction of figure 2 of Chen & Sreenivasan (2022) [3]; note that the key to symbols in parts (c) and (d) are based on parts (a) and (b): The Re_τ -variations of peak turbulence intensities. Streamwise intensity $u_p'^2$ in channel and pipe (a), and in TBL (b). Spanwise intensity $w_p'^2$ in channel and pipe (c), and in TBL (d). Newly included data are: EXP pipes of Princeton by Hultmark et al. (2012) [7], of CICLoPE by Willert et al. (2017) [8] based on PIV measurement, and by Fiorini (2017) [9] with hot-wire data corrected; DNS data of pipes by Ahn et al. (2015) [10] and of channels by Yao, Chen & Hussain (2019) [11]; EXP data of TBL by DeGraaff & Eaton (2000) [12], Örlü (2009) [13], Vincenti et al. (2013) [14], Marusic et al. (2015) [15], Vallikivi et al. (2015) [16] and Samie et al. (2018) [17]; see figure legends for the corresponding symbols. Solid lines are fit to equation (2.2)[3], whose parameters are summarized in table 1[3] Dashed lines indicate $u_p'^2 = 0.63 \ln(Re_\tau) + 3.8$ by Marusic et al. (2017) [18], and $w_p'^2 = 0.46 \ln(Re_\tau) - 1.2$ adopted by us for reference, both of which arise from the Gaussian-logarithmic model for high-order moments, as discussed in the text and shown in figures 4 and 5 of Chen & Sreenivasan [3].

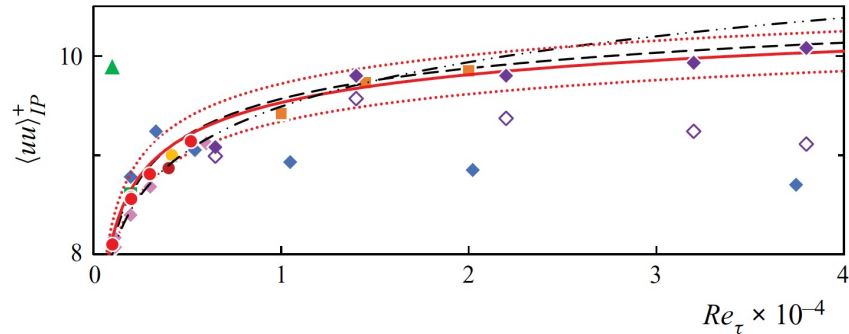


FIG. 5: Reproduction of figure 2 of Monkewitz (2022) [2]: Inner peak height $\langle uu \rangle_{IP}^+$ vs. Re_τ : (red) —, \dots , (equation 2.4 in [2]) $\pm 2\%$; (black) - - -, $11.5 - 19.3 Re_\tau^{-0.25}$ of [3]; (black) - · - ·, $3.54 + 0.646 \ln Re_\tau$ of Samie et al. (2018) [17] Channel DNS (circle): (red) DNS of table 1, (dark red) DNS of Bernardini, Pirozzoli & Orlandi (2014) [19], (yellow) DNS of Lozano-Durán & Jiménez (2014)[20] Pipe (diamond): (pink) DNS of Pirozzoli et al. (2021) [21], (blue) Superpipe NSTAP data of Hultmark et al. (2012) [7], (purple) corrected and uncorrected (open diamond) CICLoPE hot-wire data of Fiorini (2017) [9] ZPG TBL (square): (green) Sillero, Jiménez & Moser (2013) [22], (orange) Samie et al. (2018) [17] Couette (triangle): (green) Kraheberger et al. (2018) [23].

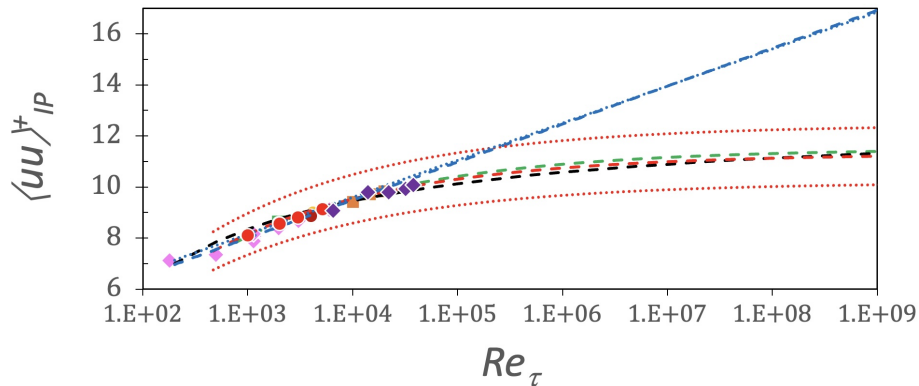


FIG. 6: Comparison between trends of peak streamwise normal stress over wide range of Reynolds numbers (data from figure 5 excluding Couette [23], NSTAP [7] and uncorrected Fiorini [9] results), and projections of equation 3 (black - - -) based on Monkowitz & Nagib (2015) [4], relation $\langle uu \rangle_P^+ = 11.5 - 19.3 Re_\tau^{-0.25}$ of Chen & Sreenivasan (2022) [3] (green - - -), and equation 2 of Monkewitz (2022) [2] (red - - - & $\pm 10\%$ \cdots), demonstrating that three proposed trends are in agreement. The proposed relations of Marusic et al. (2015) [15], equation 5 (blue - - -), and Samie et al. (2018) [17], equation 8 (blue \cdots), deviate from agreement with other relations for $Re_\tau > 50,000$.

Conclusions: Remarkable agreement is found in figure 6 over range $10^3 < Re_\tau < 10^9$ among the trends of the three proposed relations: Monkewitz (2022) [2] (equation 2), the relation $\langle uu \rangle_P^+ = 11.5 - 19.3 Re_\tau^{-0.25}$ of Chen & Sreenivasan (2022) [3], and the relation of Monkewitz & Nagib (2015) [4] with modified coefficients. The exception is the trend based on attached eddy model reported by Marusic et al. (2017) [15] and by Samie et al. (2018) [17] in equation 5, both of which start to depart from other relations near $Re_\tau = 50,000$. While Re_τ of neutral atmospheric boundary layers do exceed 10^5 , the uncertainty in the measurements does not render them useful to resolve the question of the asymptotic limit. Thus we conclude that only wall-bounded turbulent flows with $Re_\tau > O(10^6)$, using accurate measurements of $\langle uu \rangle_P^+$, can clearly and directly distinguish between recently proposed trends of the peak in streamwise normal stress profiles, i. e., $\langle uu \rangle_{IP}^+$.

Accurate measurements of high-order moments [3, 6], with guidance from consistent asymptotic expansions, see, e.g., Monkewitz (2023) [26], will be helpful in resolving the issue on hand. Such diagnostics have been developed recently by Chen & Sreenivasan (2024) [27], who have made detailed comparisons between the saturation formulae for high-order moments and experimental and DNS data. These comparisons show that the saturation forms are superior to the logarithmic formulae. Establishing which of the two approaches is more valid is not only significant for estimating the streamwise normal stresses in the high Reynolds numbers range, but also for the fundamental understanding of many aspects of wall-bounded turbulence.

What appears clear is also that the logarithmic and power scalings discussed earlier are mutually exclusive. This is seen by considering the transformation between competing large Reynolds number expansions of any quantity F_i in terms of $\ln Re_\tau$ and of $Re_\tau^{-\gamma}$:

$$\left\{ \begin{array}{l} F_i = f_1^{\log} \ln Re_{\tau,i} + f_2^{\log} \quad i = 1, 2 \\ F_i = f_1^{\text{pow}} + f_2^{\text{pow}} Re_{\tau,i}^{-\gamma} \quad i = 1, 2 \end{array} \right\}, \quad f_1^{\log}(y^+) = f_2^{\text{pow}}(y^+) \frac{Re_{\tau,1}^{-\gamma} - Re_{\tau,2}^{-\gamma}}{\ln Re_{\tau,1} - \ln Re_{\tau,2}}. \quad (8)$$

It follows that the coefficient $f_1^{\log}(y^+)$ of $\ln Re_\tau$ in the logarithmic expansion goes to zero for any positive γ , as the two $Re_{\tau,i}$ in equation 8 become large.

REFERENCES

-
- [1] H. Nagib, K. Chauhan, and P. Monkewitz, Approach to an asymptotic state for zero pressure gradient turbulent boundary layers, *Phil. Trans. R. Soc. A* **365**, A755 (2007).
- [2] P. Monkewitz, Asymptotics of streamwise reynolds stress in wall turbulence, *J. Fluid Mech.* **931**, A18 (2022).
- [3] X. Chen and K. R. Sreenivasan, Law of bounded dissipation and its consequences in turbulent wall flows, *J. Fluid Mech.* **933**, A20 (2022).
- [4] P. Monkewitz and H. Nagib, Large-reynolds-number asymptotics of the streamwise normal stress in zero-pressure-gradient turbulent boundary layers, *J. Fluid Mech.* **783**, 101688 (2015).
- [5] I. Marusic and J. Monty, Attached eddy model of wall turbulence, *Annu. Rev. Fluid. Mech.* **51**, 49 (2019).
- [6] X. Chen and K. R. Sreenivasan, Reynolds number asymptotics of wall-turbulence fluctuations, *J. Fluid Mech.* , Accepted for publication (2023).
- [7] M. Hultmark, M. Vallikivi, S. C. C. Bailey, and A. J. Smits, Turbulent pipe flow at extreme reynolds numbers, *Phys. Rev. Lett.* **108**, 094501 (2012).
- [8] C. Willert, J. Soria, M. Stanislas, J. Klinner, O. Amili, M. Eisfelder, C. Cuvier, G. Bellani, T. Fiorini, and A. Talamelli, Near-wall statistics of a turbulent pipe flow at shear reynolds numbers up to 40 000, *J. Fluid Mech.* **826**, R5 (2017).
- [9] T. Fiorini, Turbulent pipe flow - high resolution measurements in ciclope, PhD thesis, University of Bologna (2017).
- [10] J. Ahn, J. H. Lee, J. Lee, J. Kang, and H. Sung, Direct numerical simulation of a 30r long turbulent pipe flow at $Re_\tau = 3008$, *Phys. Fluids* **27**, 065110 (2015).
- [11] J. Yao, X. Chen, and F. Hussain, Reynolds number effect on drag control via spanwise wall oscillation in turbulent channel flows, *Phys. Fluids* **31**, 085108 (2019).
- [12] D. DeGraaff and J. Eaton, Reynolds-number scaling of the flat plate turbulent boundary layer, *J. Fluid Mech.* **422**, 319 (2000).
- [13] R. Örlü, Experimental studies in jet flows and zero pressure-gradient turbulent boundary layers, PhD thesis, KTH, Stockholm (2009).
- [14] P. Vincenti, J. Klewicki, C. Morrill-Winter, C. White, and M. Wosnick, Streamwise velocity statistics in turbulent boundary layers that spatially develop to high reynolds number, *Exp. Fluids* **54**, 1629 (2013).
- [15] I. Marusic, K. Chauhan, K. Kulandaivelu, and N. Hutchins, Evolution of zero-pressure-gradient boundary layers from different tripping conditions, *J. Fluid Mech.* **783**, 379 (2015).
- [16] M. Vallikivi, B. Gamathisubramani, and A. Smits, Spectral scaling in boundary layers and pipes at very high reynolds numbers, *J. Fluid Mech.* **771**, 303 (2015).
- [17] M. Samie, I. Marusic, N. Hutchins, M. Fu, Y. Fan, M. Hultmark, and A. Smits, Fully resolved measurements of turbulent boundary layer flows up to $Re_\tau = 20000$, *J. Fluid Mech.* **851**, 391 (2018).
- [18] I. Marusic, W. Baars, and N. Hutchins, Scaling of the streamwise turbulence intensity in the context of inner-outer interactions in wall turbulence, *Phys. Rev. Fluids* **2**, 100502 (2017).
- [19] M. Bernardini, S. Pirozzoli, and P. Orlandi, Velocity statistics in turbulent channel flow up to $Re_\tau = 4000$, *J. Fluid Mech.* **758**, 327 (2014).
- [20] A. Lozano-Durán and J. Jiménez, Effect of the computational domain on direct simulations of turbulent channels up to $Re_\tau = 4200$, *Phys. Fluids* **26**, 011702 (2014).
- [21] S. Pirozzoli, J. Romero, M. Fatica, R. Verzicco, and P. Orlandi, One-point statistics for turbulent pipe flow up to $re_\tau \approx 6000$, *J. Fluid Mech.* **926**, A28 (2021).
- [22] J. Sillero, J. Jiménez, and R. D. Moser, One-point statistics for turbulent wall-bounded flows at Reynolds numbers up to $\delta^+ \approx 2000$, *Phys. Fluids* **25**, 105102 (2013).
- [23] S. Kraheberger, S. Hoyas, and M. Oberlack, Dns of a turbulent couette flow at constant wall transpiration up to $Re_\tau = 1000$, *J. Fluid Mech.* **835**, 421 (2018).
- [24] H. Nagib, R. Vinuesa, and S. Hoyas, Utilizing indicator functions with computational data to confirm nature of overlap in normal turbulent stresses: logarithmic or quarter-power, arXiv:2405.14675v1, to appear in *Phys. Fluids* **36** (2024).
- [25] L. Smits, M. Hultmark, M. Lee, S. Pirozzoli, and X. Wu, Reynolds stress scaling in the near-wall region of wall-bounded flows, *J. Fluid Mech.* **926**, A31 (2021).
- [26] P. Monkewitz, Reynolds number scaling and inner-outer overlap of stream-wise reynolds stress in wall turbulence, arXiv:2307.00612v3 (2023).
- [27] X. Chen and K. R. Sreenivasan, Bounded asymptotics for high-order moments in wall turbulence, arXiv:2406.18711v1 (2024).